

Contents

2020-12-15 Daily dataset Jan 1993 - Mar 2020	2
Statistical analysis on the Mesoscale Eddy Trajectory Atlas Product	2
Introduction	2
Rationale	2
The AVISO+ Eddy Atlas in a few words	2
Figure 2	3
Figure 3	4
Figure 3 curviligne distance	5
Figure 4ab	6
Figure 4cd	7
Figure 4ef	8
Figure 5a + Figure 8	9
Figure 6	10
Figure 9	11
Figure 10	13
Figure 11	14
Figure 12	15
Figure 13	16
Figure 12_U	17
Figure 16a	18
Figure 16b	19
Figure 18	20
Figure 20	21
Figure 24	22

2020-12-15 Daily dataset Jan 1993 - Mar 2020

Statistical analysis on the Mesoscale Eddy Trajectory Atlas Product

Introduction

This document includes a series of figures showing census statistics about the eddies identified and tracked. These figures, computed and plotted from the new dataset can be compared with the figures in Chelton et al. [2011]. They are numbered identically to compare as easily as possible the characteristics of the eddies in the new eddy dataset with the eddies in the old dataset. No specific comment nor interpretation are given in the legends. For explanations and discussion, see the original article.

Dudley B. Chelton, Michael G. Schlax, Roger M. Samelson, 2011: Global observations of nonlinear mesoscale eddies, *Progr. Oceanogr.*, 91 (2011) 167–216, doi:10.1016/j.pocean.2011.01.002

Rationale

The mesoscale circulation is defined like a class of energetic phenomena of spatial scales ranging from about ten to several hundred kilometers and time scales ranging from a few days to several months. Its forcing mechanisms are mainly instabilities from the large-scale circulation and interactions between currents and bathymetry and the direct forcing by the wind.

Altimetry enables observations of such phenomena by measuring the sea surface topography around which currents swirl by the geostrophic balance between the pressure gradient force and the Coriolis acceleration. A best resolution is obtained with several satellites to study and understand eddies, with diameters ranging from 100 to 300 km (when the ground track separation at equator is about 315 km for Jason). The existence of at least two satellites operating simultaneously is therefore necessary for this type of research.

Analysis of Sea Level Anomalies from merged satellite data reveals the areas of high eddy activity, the number of eddies during those years, their horizontal scale and height. Such a census helps understanding ocean dynamics due to eddies, and to discriminate eddies' effect from other processes (like the Rossby waves). This reveals that most of the mesoscale features are “non-linear”, i.e. that these features are coherent structures (as opposed to planetary waves that would be linear). Moreover, nearly all of those eddies can transport heat, salts and nutrients trapped within them – also as opposed to planetary waves that would not transport water parcels. There are more anticyclonic eddies in some regions (positive sea level anomalies), like the Tehuantepec and Papagayo eddy area, others more cyclonic eddies, such as seen in the Humboldt Current.

The AVISO+ Eddy Atlas in a few words

A dedicated dataset has been produced, for the 16-year period October 1992 - December 2008 by Chelton et al. in 2011 at Oregon State University [Chelton et al., 2011] with a weekly time step, thus enabling easy statistics and long-term studies. Each eddy was defined on the basis of connected pixels that satisfy specified criteria. The procedure was a 2-dimensional version of the method presented by Williams et al. [2011], modified as described by Schlax and Chelton (2016).

The detection and tracking algorithm have been adapted in collaboration between D. Chelton and CLS/DUACS. The major changes compared to the original dataset [Chelton et al., 2011] are the daily input SLA fields used now for the detection step, an improved filtering to remove the large scale, and the restriction of the day-to-day maximum distance allowed during the tracking step to avoid large jumps in eddy location.

The eddy atlas is now routinely generated and quality-controlled by the DUACS team and distributed by AVISO+.

Figure 2

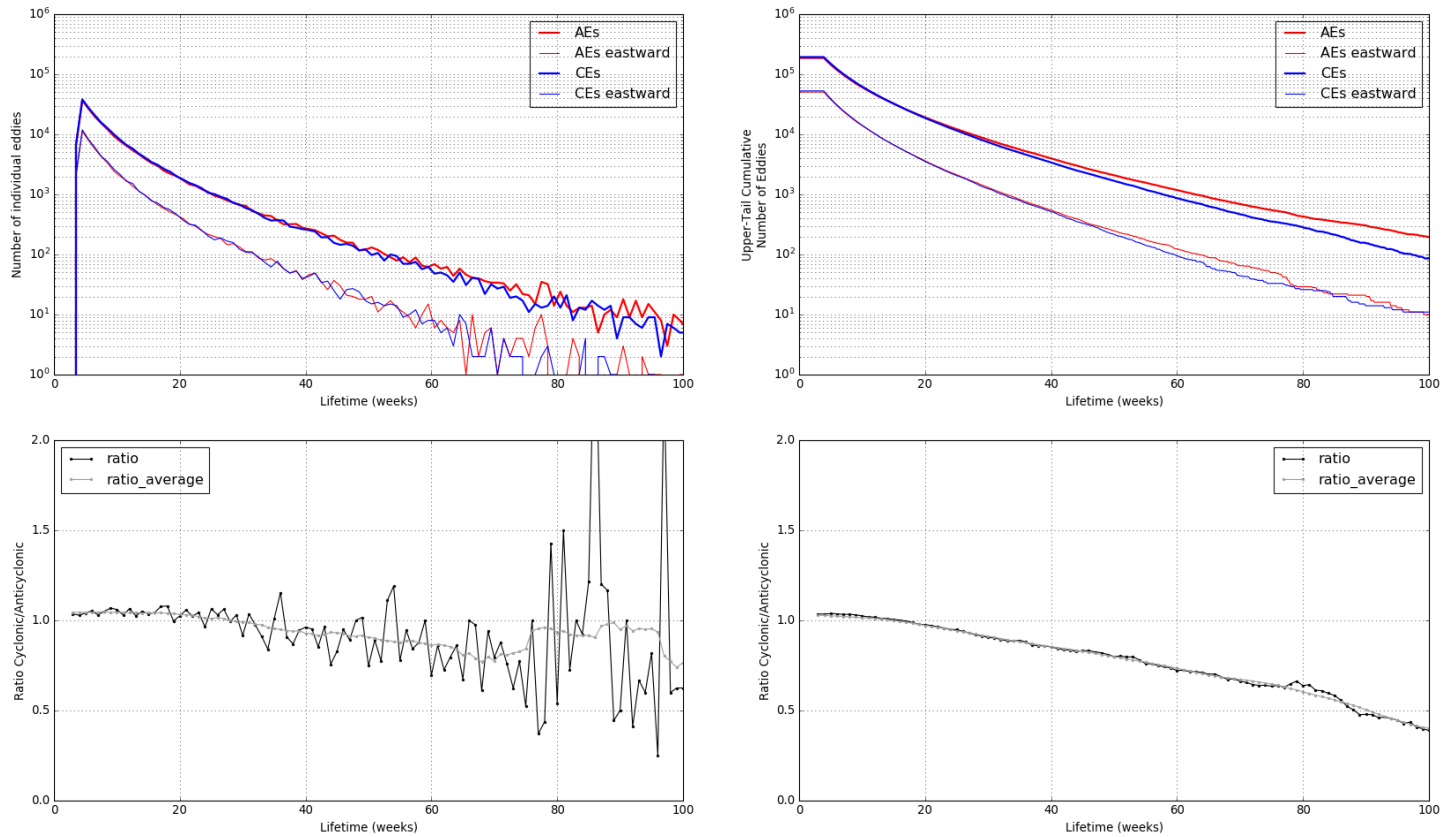


Figure 2 Histograms (left) and upper-tail cumulative histograms (right) of the lifetimes of the cyclonic (blue lines) and anticyclonic (red lines) eddies over the 27-years period January 1993 - March 2020. The ratios of these histogram values are shown by the black lines in the bottom panels and the grey lines in the bottom panels are 21-week running averages of the ratios. (The two lines are almost indistinguishable in the ratio of the upper-tail cumulative histograms.) The thin lines in the top panels are for only those cyclonic (blue lines) and anticyclonic (red lines) eddies for which the net displacement was eastward. Note : some variations with the figures in Chelton et al. (2011) can be found. They are due to the choice of the bin edges : (0, 1, 2, ...) here and (0.5, 1.5, 2.5, ...) for D. Chelton's figures

Figure 3

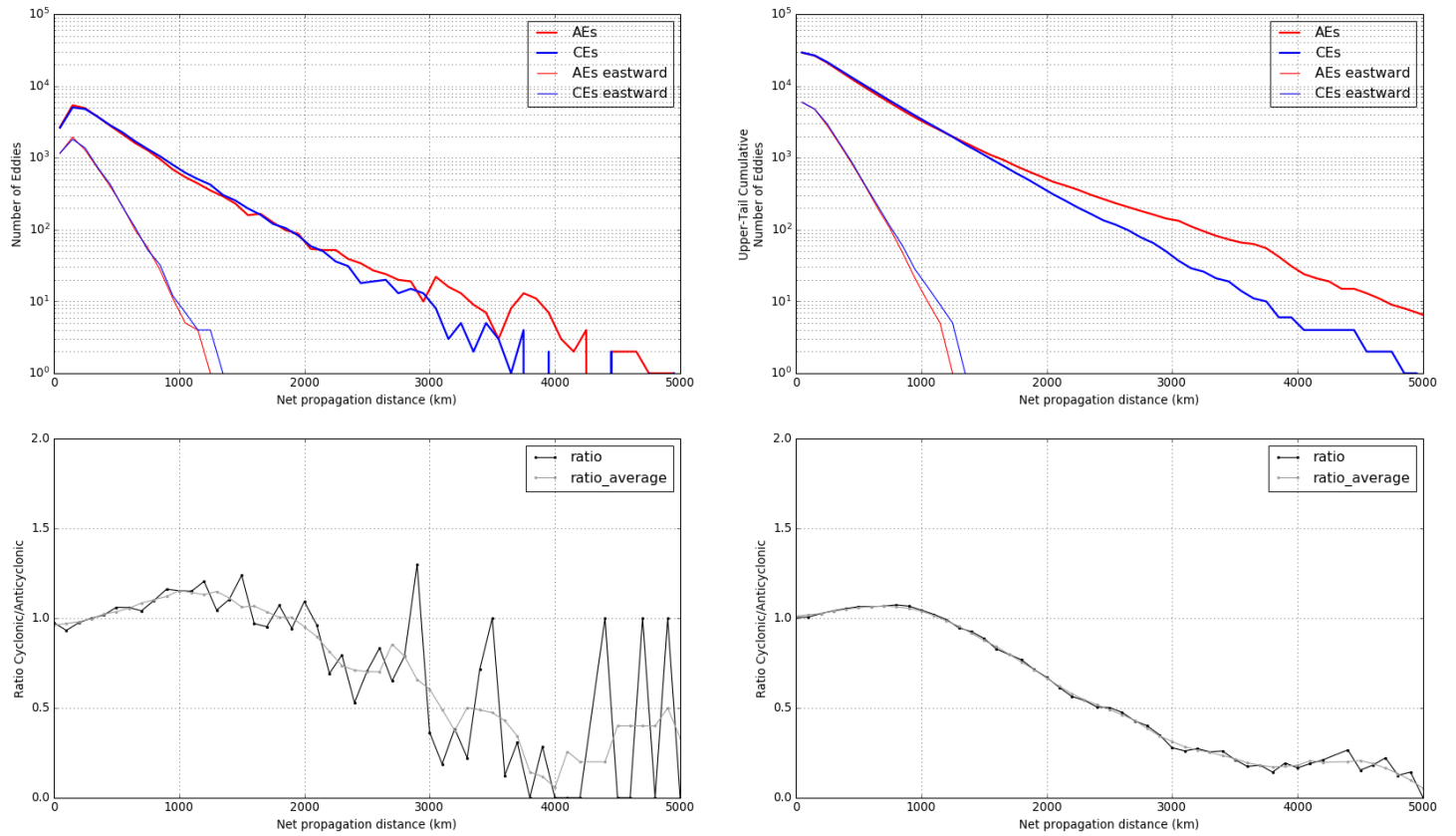


Figure 3 Histograms (left) and upper-tail cumulative histograms (right) of the great-circle propagation distances of cyclonic (blue lines) and anticyclonic (red lines) eddies with lifetimes ≥ 16 weeks over the 27-years period January 1993 - March 2020. The ratios of these histogram values are shown by the black lines in the bottom panels and the grey lines in the bottom panels are 500-km running averages of the ratios. (The two lines are almost indistinguishable in the ratio of the upper-tail cumulative histograms.) The thin lines in the top panels are for only those cyclonic (blue lines) and anticyclonic (red lines) eddies for which the net displacement was eastward.

Figure 3 curviligne distance

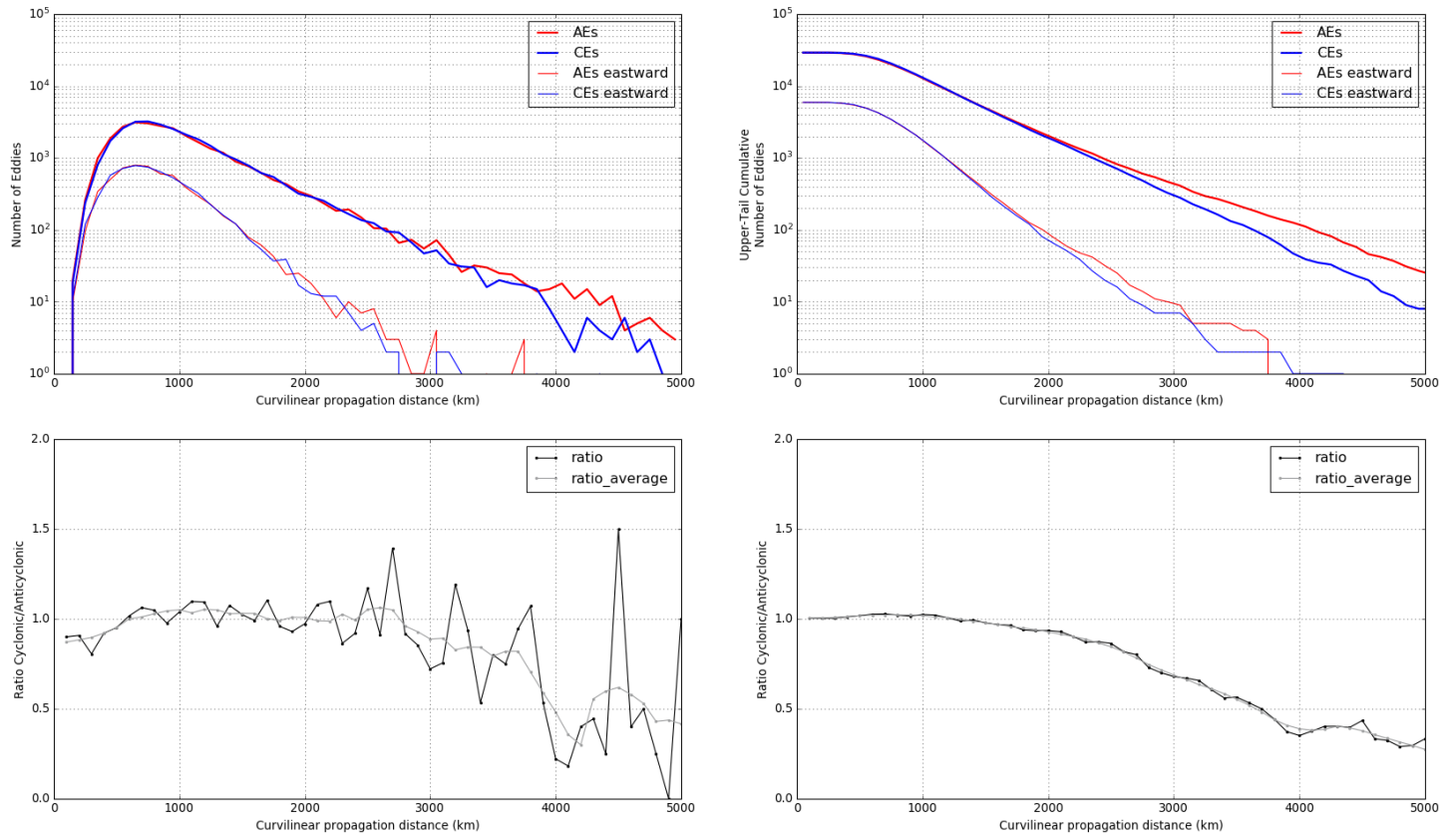


Figure 3 curviligne distance Histograms (left) and upper-tail cumulative histograms (right) of the curvilinear great-circle propagation distances of cyclonic (blue lines) and anticyclonic (red lines) eddies with lifetimes ≥ 16 weeks over the 27-years period January 1993 - March 2020. The ratios of these histogram values are shown by the black lines in the bottom panels and the grey lines in the bottom panels are 500-km running averages of the ratios. (The two lines are almost indistinguishable in the ratio of the upper-tail cumulative histograms.) The thin lines in the top panels are for only those cyclonic (blue lines) and anticyclonic (red lines) eddies for which the net displacement was eastward.

Figure 4ab

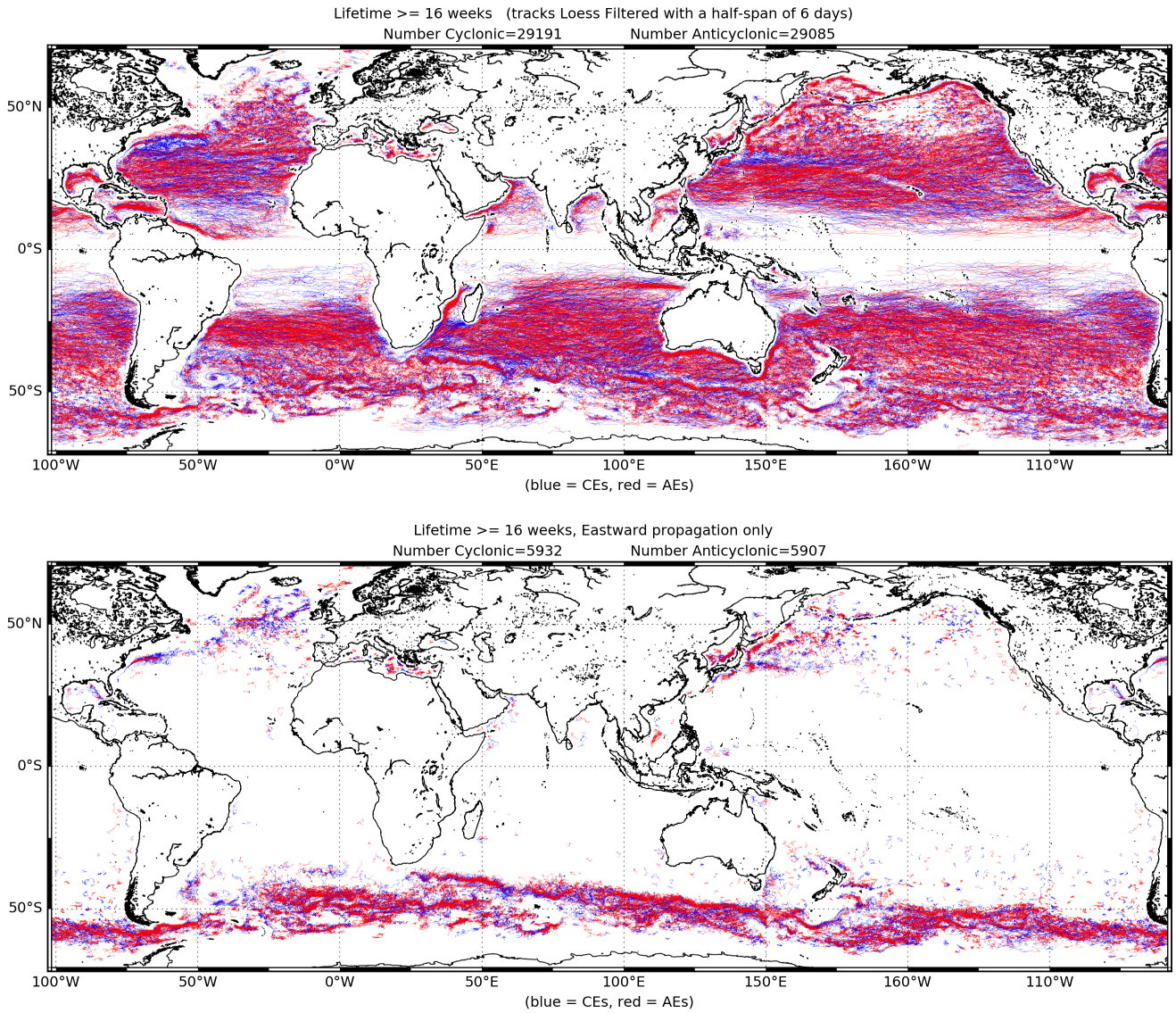


Figure 4a and b The trajectories of cyclonic (blue lines) and anticyclonic (red lines) eddies over the 27-years period January 1993 - March 2020 for a) lifetimes ≥ 16 weeks; and b) lifetimes ≥ 16 weeks for only those eddies for which the net displacement was eastward. The numbers of eddies of each polarity are labeled at the top of each panel.

Figure 4cd

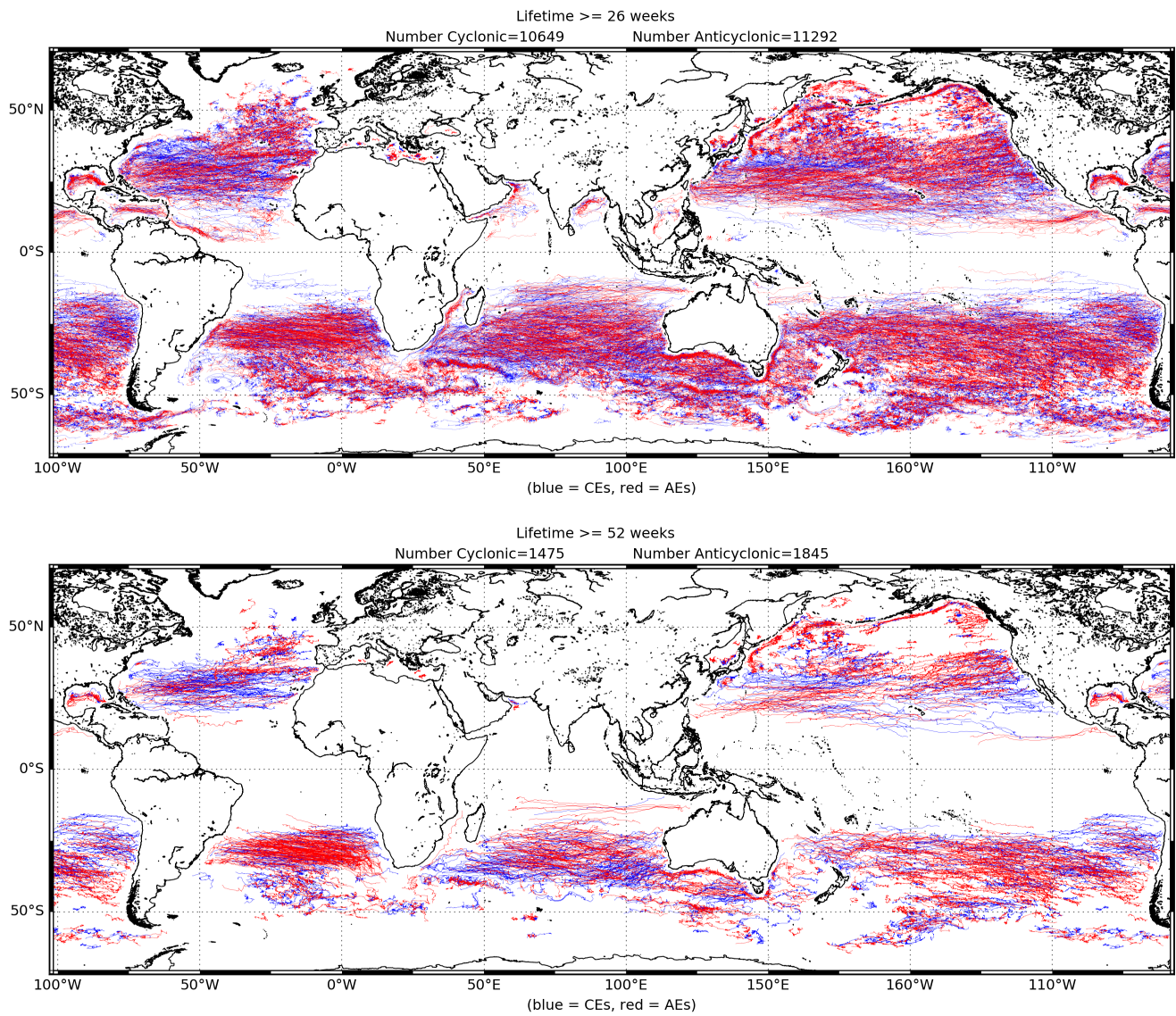


Figure 4c and d. The same as Fig. 4a, except: c) lifetimes ≥ 26 weeks; and d) lifetimes ≥ 52 weeks.

Figure 4ef

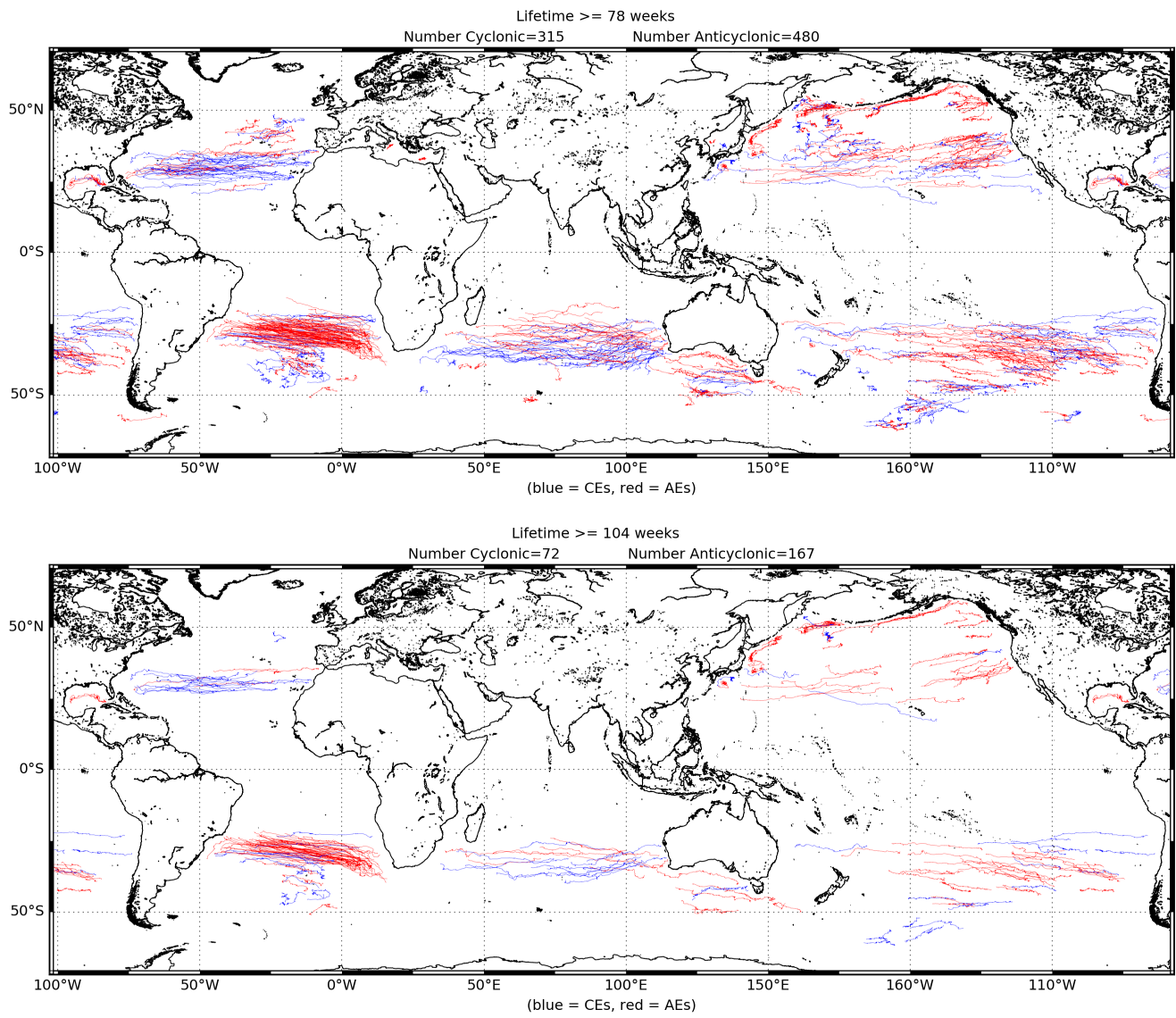


Figure 4e and f The same as Fig. 4a, except: e) lifetimes ≥ 78 weeks; and f) lifetimes ≥ 104 weeks.

Figure 5a + Figure 8

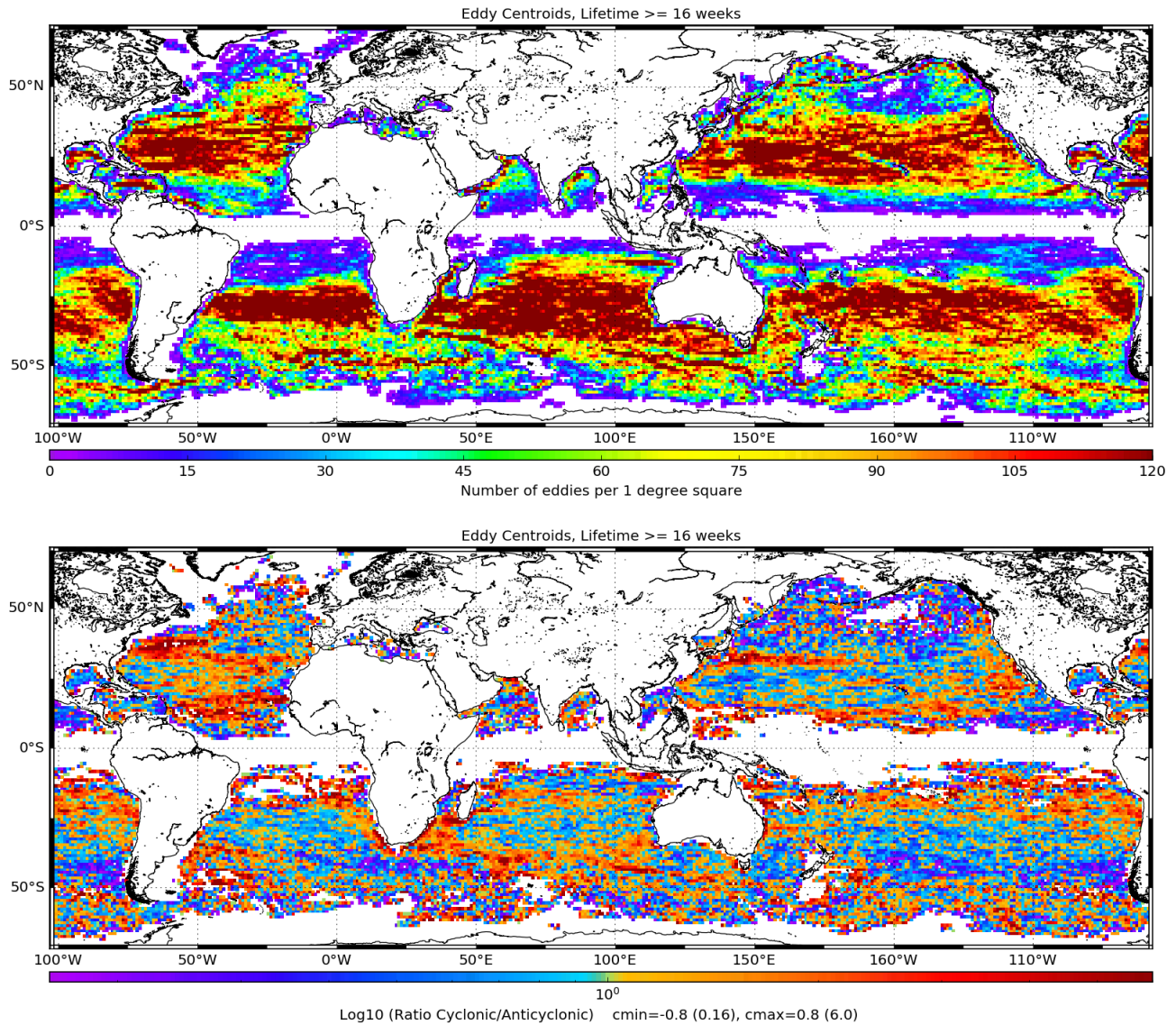


Figure 5a (upper) Census statistics for the numbers of eddy centroids for eddies with lifetimes ≥ 16 weeks (and tracks smoothed using a Loess Filter with a half-span of 6 days) that passed through each $1^\circ \times 1^\circ$ region over the 27-years period January 1993 - March 2020.

Figure 8 (lower) The ratio of the numbers of cyclonic to anticyclonic eddy centroids for eddies with lifetimes ≥ 16 weeks (and tracks smoothed using a Loess Filter with a half-span of 6 days) that propagated through each $1^\circ \times 1^\circ$ region over the 27-years period January 1993 - March 2020. A logarithmic scale is used for the color bar in order to give equal emphasis to the ratios r and $1/r$.

Figure 6

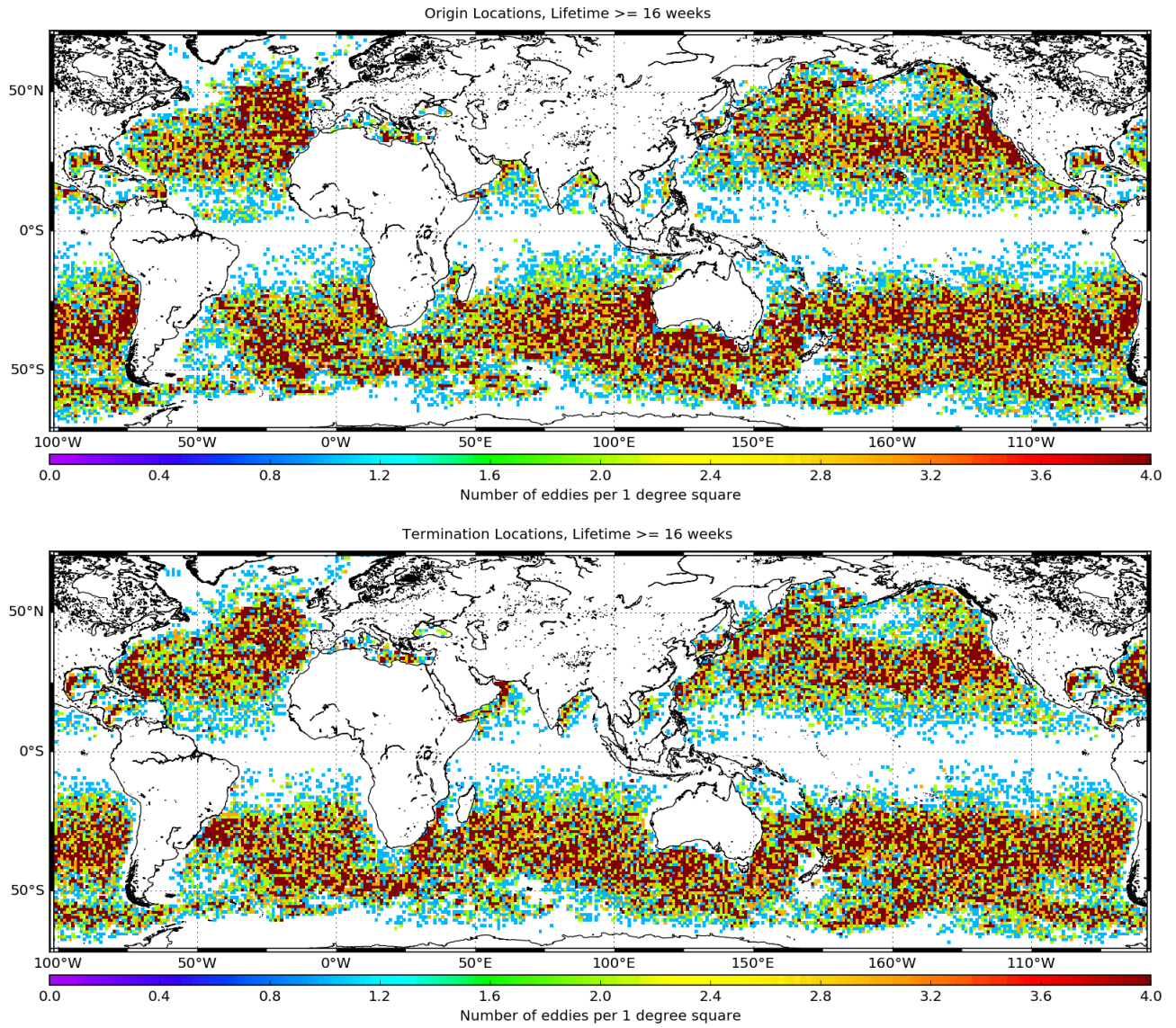
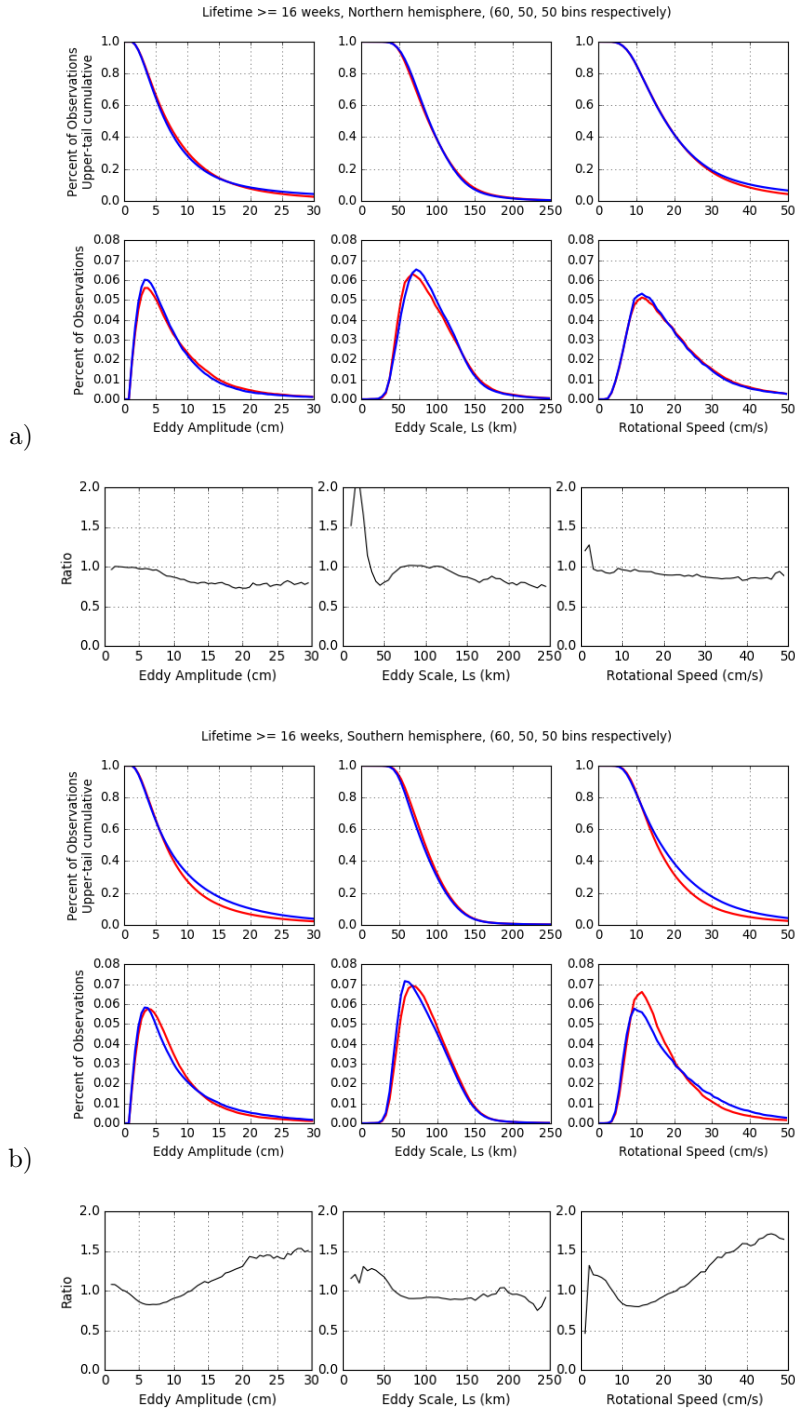
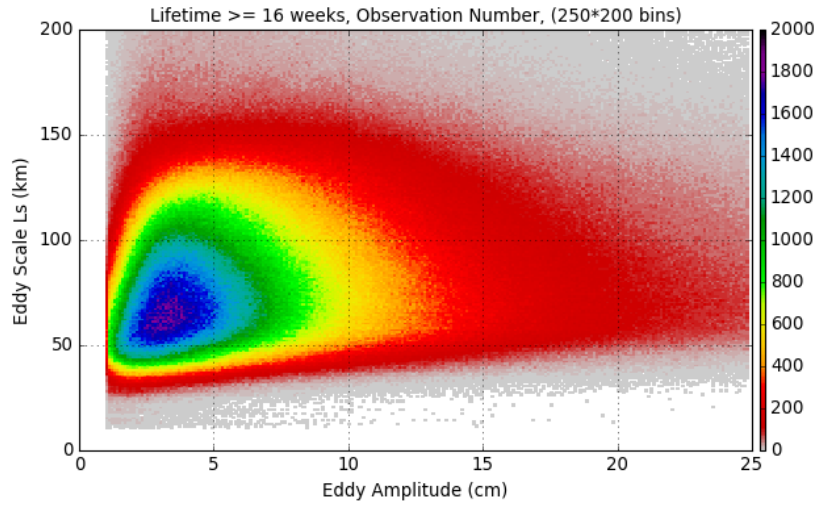


Figure 6 Census statistics for eddies with lifetimes ≥ 16 weeks showing the numbers of a) eddy origins, and b) eddy terminations, for each $1^\circ \times 1^\circ$ region over the 27-years period January 1993 - March 2020.

Figure 9





c)

Figure 9 The distributions of the amplitudes A , speed-based scale L_s , and rotational speeds U (left to right) of eddies with lifetimes ≥ 16 weeks in a) the northern hemisphere, and b) the southern hemisphere. Upper-tail cumulative histograms and histograms are shown in the first and second rows of panels, respectively, with blue and red lines corresponding, respectively, to histograms for cyclonic and anticyclonic eddies. The ratios of cyclonic to anticyclonic are shown in the third rows of panels. The global two-dimensional histogram of the joint distribution of the amplitudes A and scales L_s is shown in panel c).

Figure 10

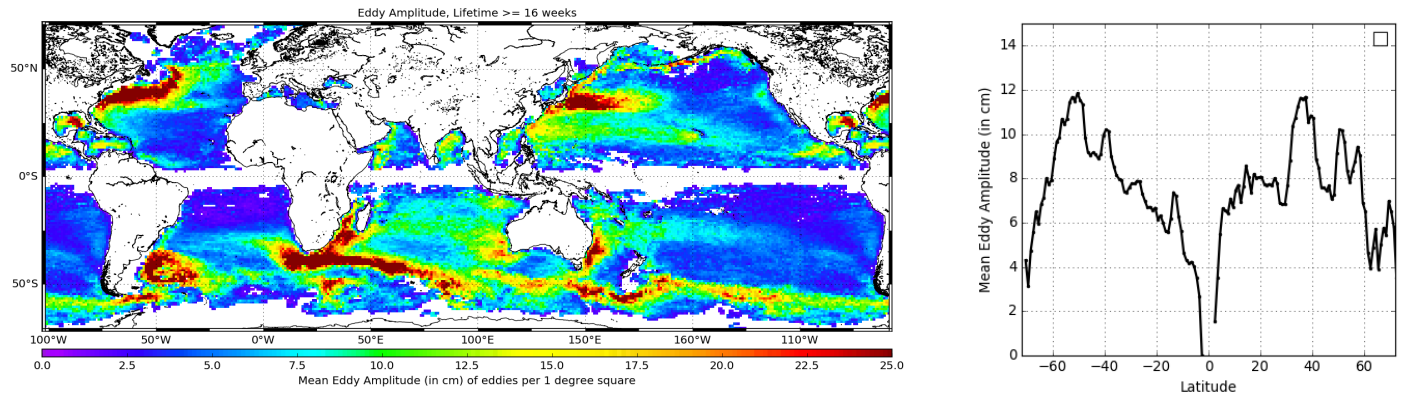


Figure 10 Maps of the average amplitude of eddies with lifetimes ≥ 16 (left) for each $1^\circ \times 1^\circ$ region. The right panel shows meridional profiles of the average of eddy amplitudes within each 1° latitude bin.

Figure 11

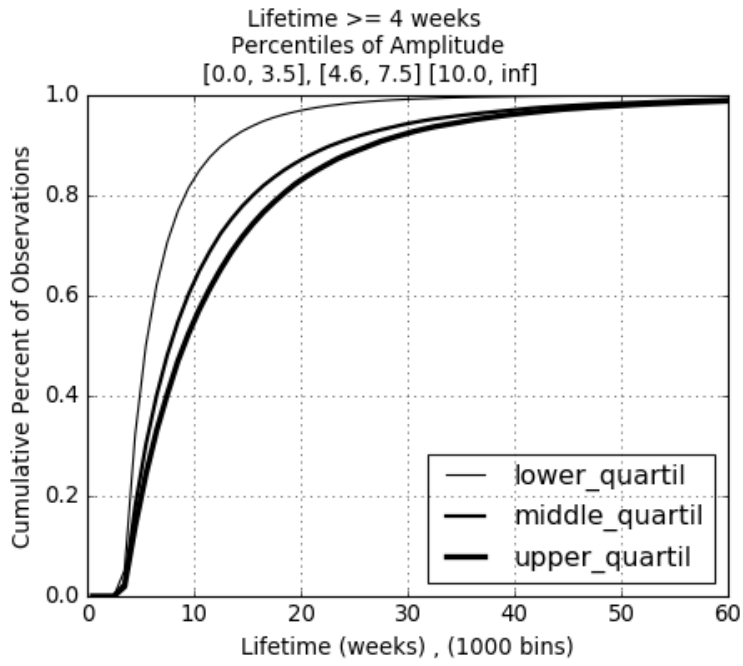


Figure 11 Cumulative histograms of the lifetime distributions of all of the tracked eddies (lifetimes ≥ 4 weeks) within the lower, middle and upper 25 percentiles of the distribution of eddy amplitudes averaged over the lifetime of each eddy: $A < 3.5$ cm (thin line), $4.6 \leq A \leq 7.5$ cm (medium line thickness), and $A > 10.0$ cm (thick line).

Figure 12

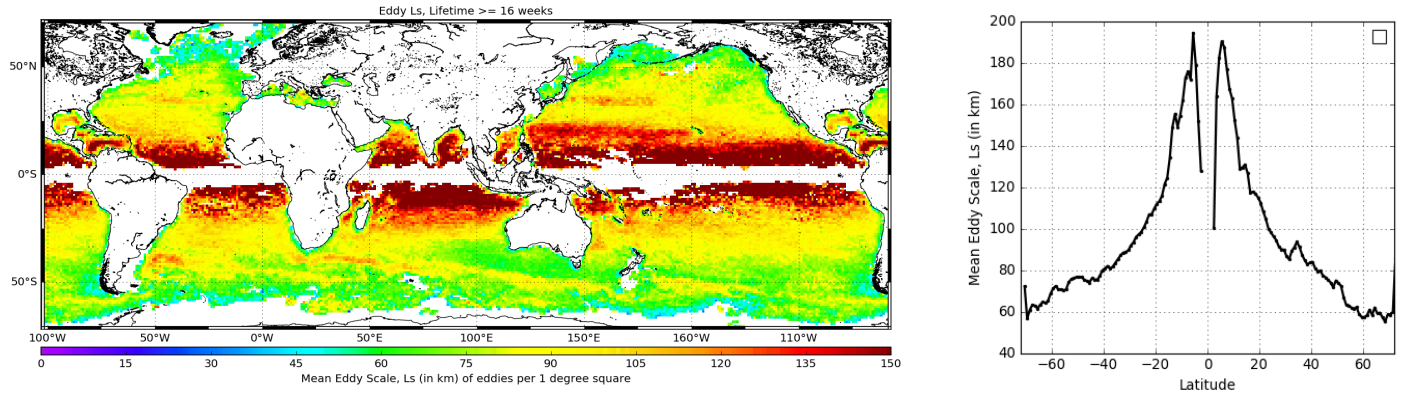


Figure 12 Map of the average speed-based eddy scale L_s for eddies with lifetimes ≥ 16 weeks (left) for each $1^\circ \times 1^\circ$ region. The right panel shows meridional profiles of L_s within each 1° latitude bin.

Figure 13

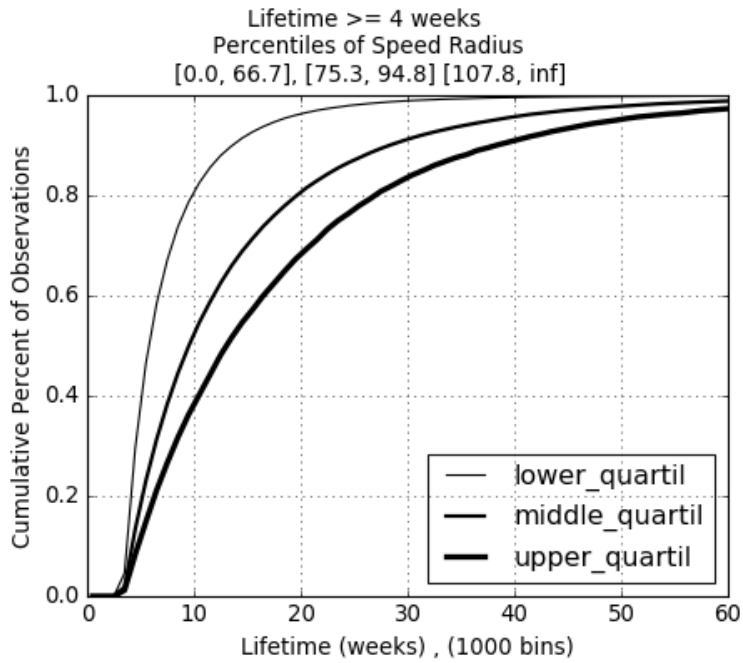


Figure 13 Cumulative histograms of the lifetime distributions of all of the tracked eddies (lifetimes ≥ 4 weeks) in the latitude range 20° to 60° of both hemispheres within the lower, middle and upper 25 percentiles of the distribution of speed-based eddy scales (averaged over the lifetime of each eddy): $L_s \leq 66.7$ km (thin line), $75.3 \text{ km} \leq L_s \leq 94.8$ km (medium line thickness), and $L_s > 107.8$ km (thick line).

Figure 12_U

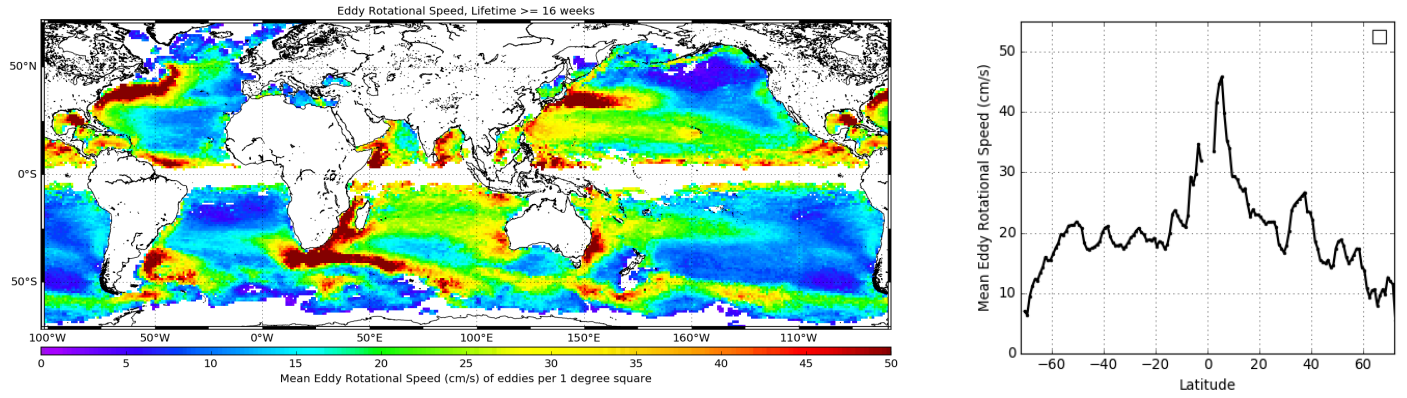


Figure 12_U Map of the average eddy rotational speed U (cm/s) for eddies with lifetimes ≥ 16 weeks (left) for each $1^\circ \times 1^\circ$ region. The right panel shows meridional profiles of U within each 1° latitude bin.

Figure 16a

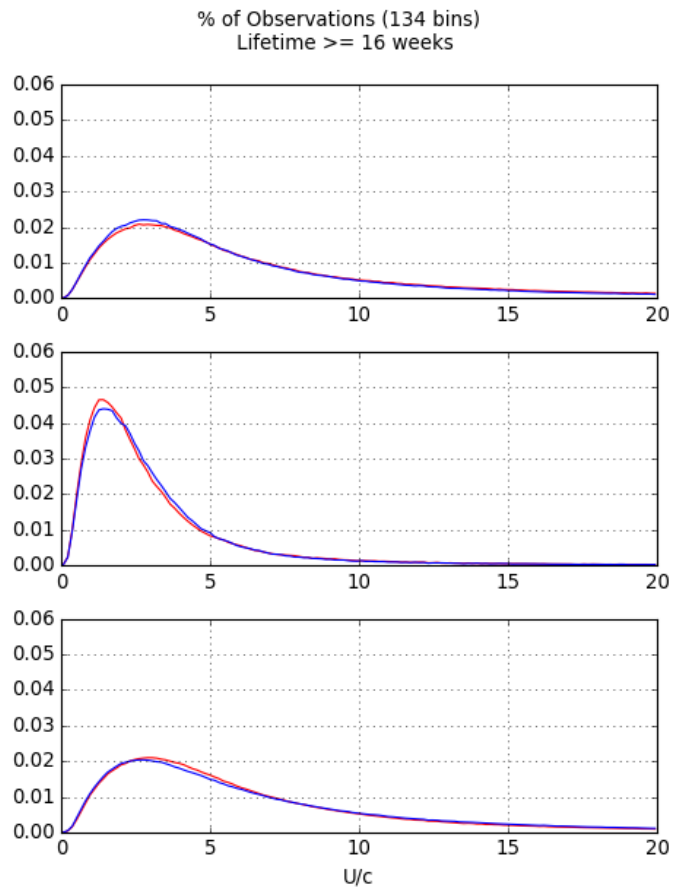


Figure 16a Histograms of the advective nonlinearity parameter U/c (c = speed of the eddy positions smoothed using a Loess filter with a 6-day half-span) of the observed mesoscale features with lifetimes ≥ 16 weeks for three different latitude bands. Top to bottom: 20°N to 60°N, 20°S to 20°N, and 60°S to 20°S. The blue and red lines in each panel correspond to cyclonic and anticyclonic eddies, respectively.

Figure 16b

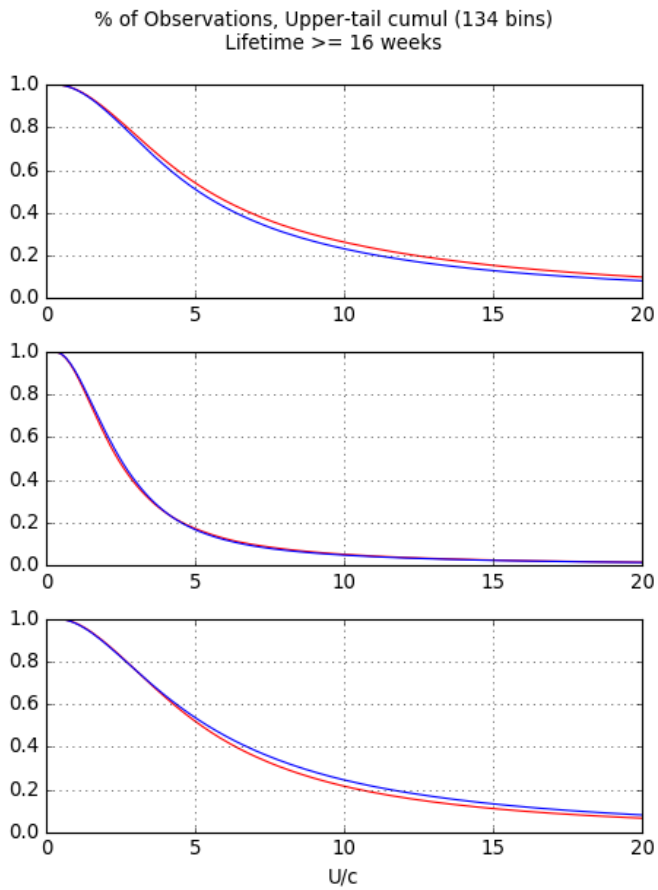


Figure 16b The same as Fig. 16a (tracks filtered with a 6 days half-span Loess Filter), except the associated upper-tail cumulative histograms for the three nonlinearity parameters in the three different latitude bands.

Figure 18

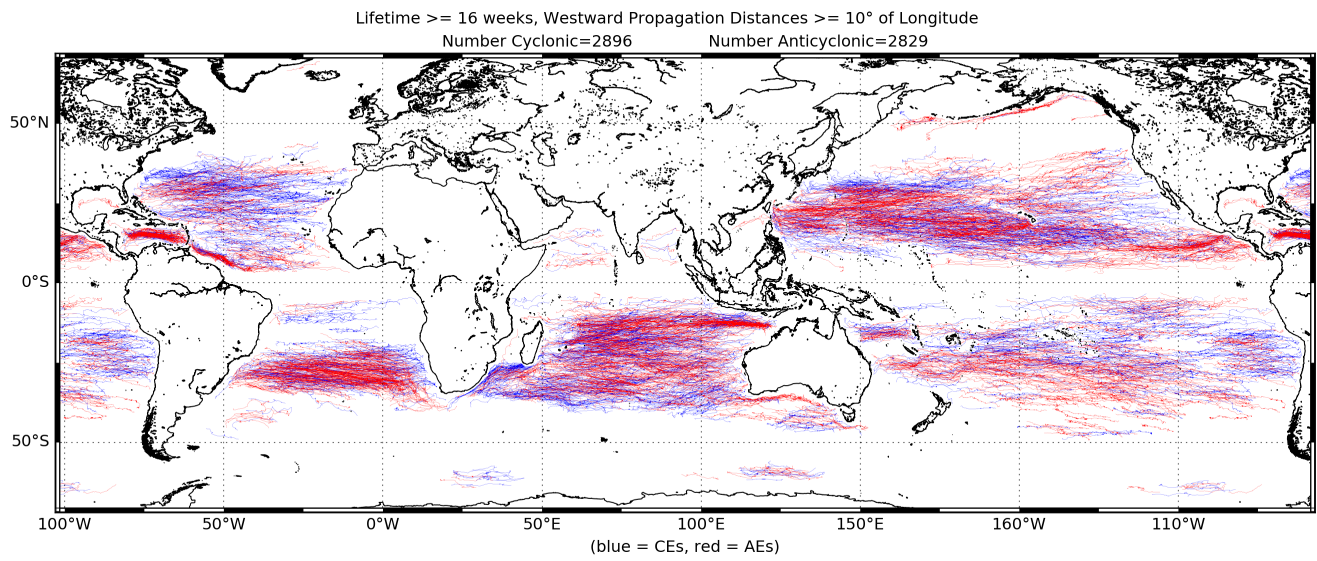


Figure 18 The trajectories of all of the cyclonic (blue lines) and anticyclonic (red lines) eddies over the 27-years period January 1993 - March 2020 that had lifetimes ≥ 16 weeks and propagated westward a minimum of 10° of longitude.

Figure 20

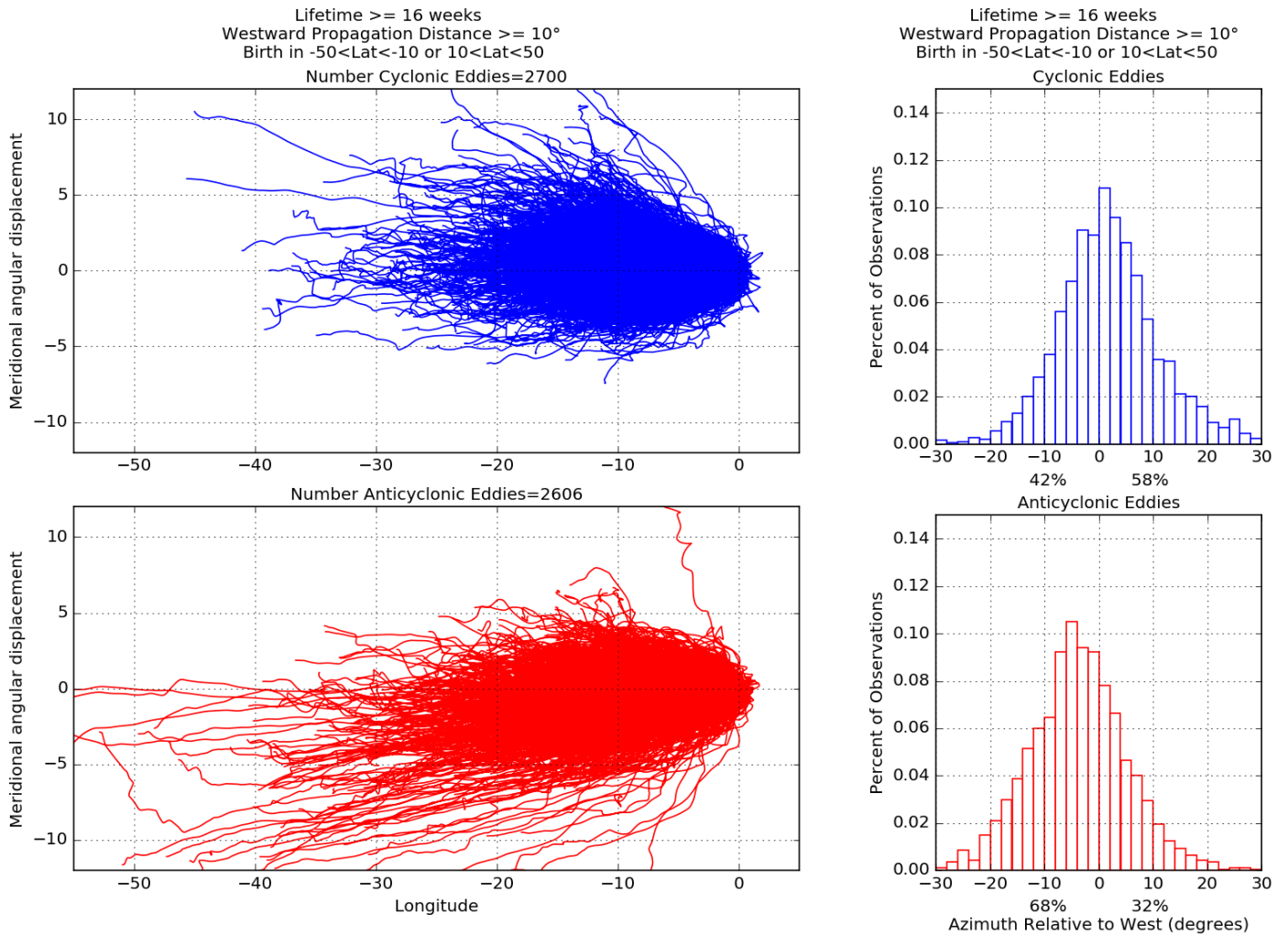


Figure 20. The meridional deflections of the cyclonic (upper panels) and anticyclonic (lower panels) eddies with lifetimes ≥ 16 weeks and starting points at latitudes between 10° and 50° of both hemispheres that propagated westward a minimum of 10° of longitude (see Fig. 18). The left panels show the changes in longitude (negative westward) and latitude (positive for poleward and negative for equatorward of due west) relative to the initial location of each eddy. The right panels show histograms of the average azimuth of each eddy trajectory (eddies with lifetimes ≥ 16 weeks), with starting points at latitudes between 10° and 50° of both hemispheres that propagated westward a minimum of 10° of longitude (see Fig. 18). The labels in the right panels indicate the percentages of negative (equatorward) and positive (poleward) eddy azimuths (eddy positions smoothed using a Loess filter with a 6-day half-span).

Figure 24

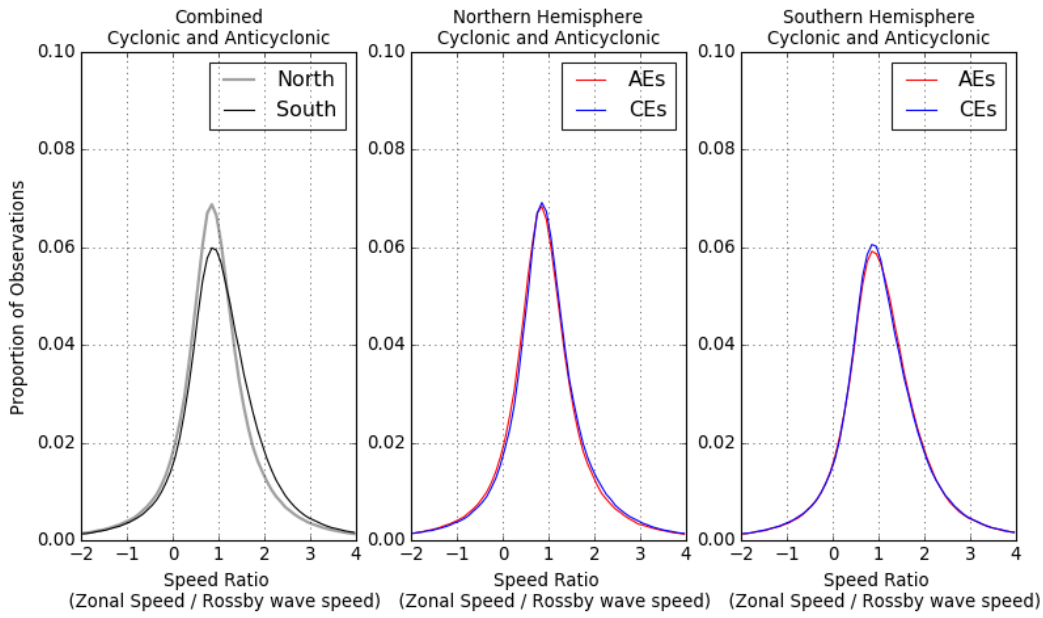


Figure 24 Distributions of eddy speeds (of the eddy positions smoothed using a Loess filter with a 6-day half-span) normalized by the local long baroclinic Rossby wave phase speed for the latitude range 15° to 40° . The distributions for cyclonic and anticyclonic eddies combined are shown in the *left* panel for the northern and southern hemispheres as grey and black lines, respectively. The distributions for cyclonic and anticyclonic eddies (blue and red lines, respectively) are shown separately for the northern and southern hemisphere in the *middle* and the *right* panels respectively.